

FISSION IN EXOTIC NUCLEI USING DENSITY FUNCTIONAL THEORY

By

Zachary Matheson

A DISSERTATION

Submitted to
Michigan State University
in partial fulfillment of the requirements
for the degree of

Physics — Doctor of Philosophy
Computational Mathematics, Science and Engineering — Dual Major

2019

ABSTRACT

FISSION IN EXOTIC NUCLEI USING DENSITY FUNCTIONAL THEORY

By

Zachary Matheson

This is my abstract.

Dedicated to I dunno

ACKNOWLEDGMENTS

I dunno who to acknowledge, either

TABLE OF CONTENTS

LIST OF FIGURES	vii
Chapter 1 Introduction	1
1.1 History of Fission Theory	1
1.1.1 Liquid Drop Model	1
1.1.2 Strutinsky shell correction	1
1.1.3 Self-consistent models and the supercomputing era	1
1.2 Goals of the project	6
Chapter 2 Describing Fission Using Nuclear Density Functional Theory	8
2.1 Nuclear Density Functional Theory	9
2.1.1 Density Functional Theory	10
2.1.1.1 Kinetic term	13
2.1.1.2 Coulomb interaction	13
2.1.1.3 Skyrme interaction	14
2.1.1.4 Pairing interaction	14
2.1.2 Bogoliubov transformation	15
2.1.3 Hartree-Fock-Bogoliubov Equations	16
2.1.4 Nucleon localization function	17
2.2 Microscopic Description of Nuclear Fission	18
2.2.1 Potential Energy Surfaces	18
2.2.2 Collective inertia	19
2.2.3 WKB Approximation	20
2.2.4 Langevin Dynamics	21
Chapter 3 Two fission modes in ^{178}Pt	22
3.1 Asymmetric fission in the region of ^{180}Hg	22
3.2 Multimode fission of ^{178}Pt	24
3.3 The physical origin of fragment asymmetry in the region of ^{180}Hg	26
Chapter 4 Cluster decay in ^{294}Og	29
4.1 Cluster emission in Superheavy Elements	29
4.2 Predicted spontaneous fission yields of ^{294}Og	31
4.3 ^{294}Og	35
4.3.1 Cluster Decay	37
4.3.2 Competition with Alpha Decay or Half-lives	37
4.4 Method	37
4.5 Experimental efforts to find cluster emission in ^{294}Og	38
Chapter 5 R-process	40

Chapter 6	Fragment Identification	43
6.1	Fragments and the Nucleon Localization Function	43
6.2	The problem of scission	44
6.3	Prefragment shell structure	45
Chapter 7	Outlook	47
7.1	Review, outlook, and perspectives	47
APPENDIX		50
.1		51
BIBLIOGRAPHY		52

LIST OF FIGURES

Figure 3.1:	Survey of fragment yields near ^{180}Hg	24
Figure 3.2:	^{178}Pt experimental data	25
Figure 3.3:	UNEDF1-HFB potential energy surface for ^{178}Pt	26
Figure 3.4:	D1S potential energy surface for ^{178}Pt	27
Figure 4.1:	Calculated and experimental decay modes for SHE	30
Figure 4.2:	Dominant decay modes for SHE in a nuclear DFT-based framework. . .	30
Figure 4.3:	PES comparison for ^{294}Og using EDFs UNEDF1 _{HFB} , D1S, and SkM*. .	32
Figure 4.4:	N-Z fission fragment yields from ^{294}Og	33
Figure 4.5:	^{294}Og heavy fragment masses and charges.	34
Figure 4.6:	Nucleon localization visualization of ^{294}Og prefragment formation. . .	36

Chapter 1

Introduction

1.1 History of Fission Theory

Nuclear fission is the fundamental physical process by which a heavy nucleus decays to two smaller nuclei with approximately equal masses, and a proper understanding of fission is critical for applications in reactor physics, nuclear astrophysics, and stockpile stewardship. It is a highly-collective process involving all the constituent nucleons of the system, and thus since its discovery it has been described via large shape deformations of an otherwise spherical (or nearly-spherical) “drop” of nucleons.

1.1.1 Liquid Drop Model

1.1.2 Strutinsky shell correction

1.1.3 Self-consistent models and the supercomputing era

[You should probably cite the fission discovery paper(s) by Hahn and Straßmann [18] and the subsequent qualitative explanation paper by Meitner and Frisch [24], not to mention the original liquid drop paper by Weizsäcker [51] and the paper in which Bohr and Wheeler invoked the liquid drop model to describe fission quantitatively in terms of bulk properties of nuclei [10]. Finally, I might also do well to mention the spontaneous fission discovery

paper [15], which is actually just a letter to the editor of Physical Review that is only a paragraph long.] Models have grown increasingly sophisticated over time (the development of the Strutinsky shell correction to the LDM energy and the Funny Hills paper [45, 46, 11], which incorporated nuclear shell effects and explained the experimental observation that fragments were not equally-sized); however, the problem is incredibly complex. First of all, one must solve the nuclear many-body problem for a large ($A > 200$) system. Then one must describe a transition from a single body to two. The way we do each of these things is described in Chapter 2.

If you're looking for a central narrative with which to tie together your thesis, you could, of course, use the whole "making things faster" angle you've been playing so far. But I think a more enriching, exciting, and satisfying approach would be to emphasize that you are doing fission calculations for *rare* nuclei. That's cool because you work in a facility for *rare* isotopes! And it's just one of those things that is interesting and fashionable in the field in general right now. The introduction to the platinum-178 paper has a good discussion about the importance of trying to understand fission in regions of exotic isospin ratios, and how simpler models tend to be less reliable in those regions. That covers both the platinum and the r-process project motivations (at least partially), and oganesson is just interesting because of how heavy it is.

It is an exciting time to study nuclear theory; major advances are now possible thanks to a groundwork laid of nuclear theory, paired with modern supercomputers fast enough for such complicated many-body problems to be solved.

It is an exciting time to study nuclear theory; for as we now enter the supercomputer age, we are able to implement the groundwork laid over the past several decades on modern, cutting-edge, high-performance computing centers. This allows

These advances in computing come simultaneously with advances in accelerator design and technology and other advances which allow experimental nuclear physics to reach far beyond what has been done before. For instance, the Facility for Rare Isotope Beams (FRIB) at Michigan State University is projected to be able to nearly double the number of isotopes that can be produced synthetically. Together, state-of-the-art facilities for experiment and high-performance computing for theory are expected to lead to rapid advancement in our understanding of atomic nuclei.

One process which has always been a driver of nuclear physics is nuclear fission, the process by which a heavy nucleus decays into two smaller nuclei of approximately equal mass. Nuclear fission has been applied by humans in the fields of energy generation and national defense, and it has been predicted to play a major role in astrophysical environments such as neutron star mergers. There is currently a great deal of interest in understanding “rare” isotopes, or isotopes which are highly-unstable, in order to better understand such exotic phenomena as neutron star mergers, as well as to better identify physical properties which we can use to better understand the nuclei which we regularly encounter on Earth.

There are a couple of ways for a nucleus to fission. One way is by imparting some excitation energy to a fissile nucleus, such as by bombarding a nucleus with neutrons (neutron-induced fission), by creating an excited nucleus as the decay product of another isotope (beta-delayed fission) or as a compound system of two collided nuclei. Owing to the randomness of quantum mechanics, another possibility is for a nucleus in its ground state to spontaneously tunnel through a potential barrier and then emerge to form two distinct fragments (spontaneous fission). This dissertation will deal primarily/exclusively with the latter.

Fission, the fundamental process by which a single heavy nucleus splits into two smaller nuclei and a few emitted neutrons, is simple to understand qualitatively but remarkably

difficult to explain quantitatively. One could argue that nuclear fission theory has leapt forward in three major waves. The first major wave of nuclear fission theory goes back to the very beginning of the nuclear age, when George Gamow proposed and Niels Bohr and John Archibald Wheeler developed the liquid drop model in the 1930s. This model was able to successfully describe nuclear binding energies and the energetics of nuclear fission. The second wave came with Strutinsky’s microscopic correction in the late 1960s, which essentially amounted to adding a quantum mechanical correction to the liquid drop energy. This correction, based on the nuclear shell model, is added in order to better account for the added stability that occurs when a nucleus contains a “magic number” of protons and/or neutrons [45, 46, 11]. The third major wave is taking place now, heralded by the age of supercomputers. Now instead of using phenomenology and quantum corrections to describe heavy nuclei, we can use quantum many-body methods which were developed years or decades ago, but which were shelved until sufficiently-powerful computers came online in recent years.

Microscopic models (as they are called) are increasingly able to predict properties of fission fragments; however, a comprehensive description of fission fragments (including mass and fragment yields, excitation and kinetic energy distributions, angular dependence, spin, neutron emission) in a microscopic framework remains elusive. A major source of this elusiveness is due to the sheer difficulty of describing a smooth transition from one nucleus to two, a concept which is plagued with ambiguities. How can one precisely identify two distinct fragments when the wavefunctions of one fragment’s constituent nucleons may extend into the opposite fragment? And how do those correlations between nucleons affect the energetics of the resulting fragments? These are the questions to be addressed by this project.

Theoretically, making predictions about fission is challenging because, thanks to the large

number of particles involved and the complex collective interactions which take place when one system deforms and becomes two, fission calculations have an "inextinguishable thirst for computing power," as stated in [43]. Historically, most fission calculations that have been done were based on empirical formulas or phenomenological models, most notably the "microscopic-macroscopic" family of models based on Bohr's liquid-drop model (to model the bulk properties of the nucleus) with Strutinsky shell corrections (to account for quantum mechanical shell effects). These microscopic-macroscopic ("micmac") fission models are computationally fairly inexpensive, and can achieve quite satisfactory results. However, since the model is based on a phenomenological description of what is actually a quantum mechanical system, its predictive power is limited, and there is no clear way of making systematic improvements.

A more reliable approach would be to consider the individual nucleon states using some kind of quantum many-body method. For large systems with many, many particles, density functional theory (DFT) is a way to recast the Schrödinger equation involving ~ 200 particles into a simpler problem involving only a few densities and currents (see section 2.1.1). With DFT as a way of calculating nuclear properties quantum-mechanically, one can then use these self-consistent solutions to predict fission properties, such as lifetimes and fragment yields. Fortunately, a great deal of work has been done to achieve exactly this (see the review article [43]). Some of the ideas which are used were inspired by lessons learned from micmac and other, simpler models; others are unique to DFT. Our approach is described in detail in chapter 2.

The challenge, now, is to do these calculations cheaply. In every theoretical calculation, one must ask oneself "What approximations can I safely make?" and "What are the important degrees of freedom for this problem?" One may also reduce the total time-to-answer

via improvements to the computational workflow itself, such as better file handling and parallelization.

1.2 Goals of the project

By far the most commonly-studied region so far for fission has been the region of actinides near ^{235}U , which includes isotopes of uranium, plutonium, and thorium relevant for nuclear energy/reactor physics and stockpile stewardship/defense. Isotopes in this region tend to fission asymmetrically, with the larger prefragment influenced by the shell structure of ^{132}Sn and resulting in a heavy fragment distribution centered around $\sim^{140}\text{Te}$. However, recent experiments have highlighted other forms of fission which take place

Given the aforementioned recent interest in rare and exotic nuclei, we have applied our model to study spontaneous fission in exotic systems found in other regions of the nuclear chart. First, in chapter 3 we discuss bimodal fission in the neutron-deficient isotope platinum-178, which until recently was expected to fission symmetrically. Then in chapter 4 we discuss cluster radioactivity in oganesson-294, the heaviest element ever produced by humans. In chapter 5 we move to the neutron-rich side of the nuclear chart to study ..., which are expected to play a major role in the astrophysical r-process.

The calculations in chapters ?? are relatively expensive. To perform large-scale exploratory studies in other regions of the nuclear chart, it will be necessary to find ways to reduce the total computational cost of these calculations. One method, still in its infancy, offers a promising approach for identifying fission fragment distributions using a significantly-reduced potential energy surface, which is by far the biggest bottleneck in our calculations. In chapter 6, we discuss the problem of scission and present an alternative method for iden-

tifying fragments based on the nucleon localization function.

Alternatively, at the end of each chapter, we say a few words about challenges faced during the project and new physical insights gained that aren't related to the overall narrative of the chapter, but which are nevertheless useful for future model developments.

Finally, in chapter 7 we discuss the current state of the field, and, based on our experience, offer insights for guiding future developments in the field.

Chapter 2

Describing Fission Using Nuclear Density Functional Theory

(Nicolas gave a good annotated presentation in 2017 that describes some of the philosophy, as well as some of the outstanding challenges of spontaneous fission in an adiabatic framework:

https://t2.lanl.gov/fiesta2017/school/Schunck_NotesSlides.pdf)

Today there are 2 microscopic approaches to fission that are in common use: time-dependent and static (time-independent) (or 3 models: time-dependent, static, and statistical). Time-dependent approaches evolve the system in real-time. Since fission is an inherently time-dependent process, these methods offer great insight into the fission process and the characteristics of the fragments \cite{Some TDHFB papers}. However, they can only treat a single event at a time, making them impractical for estimating yields. Despite efforts such as [14], there is currently no way to obtain a full yield distribution in a time-dependent framework. Furthermore, TDHFB cannot tunnel (they break down and/or become unstable or something after too many time steps, not to mention the amount of computing time), which is a problem because spontaneous fission is fundamentally a quantum mechanical tunnelling process.

On the other hand, static approaches assume that collective motion of the nucleus is slow compared to the motion of the intrinsic particles, and this assumption is used to create a

potential energy surface in some space of collective shape coordinates. We can estimate fission yields and half-lives in these approaches (see, for instance, [39] along with our forthcoming paper on ^{294}Og \cite{???}).

Implicit in this treatment is the assumption that collective and intrinsic degrees of freedom can be decoupled, and that the time-scale associated with collective degrees of freedom is slow compared to the time-scale of intrinsic (i.e. single-particle) motions of the system. In the literature this is called adiabatic approximation \cite{???}.

Adiabaticity: For fusion reactions, N,Z equilibrium reached in $\sim 10^{-21}$ seconds, then energy/thermal equilibrium in a similar time scale, then finally mass equilibrium in $\sim 10^{-19}$ - Yuri has a slide with these time scales from his talk Monday

The adiabatic approach involves calculating a potential energy surface, and then using it to perform various dynamical calculations describing the evolution of a nucleus from ground state to scission. Since we are trying to be as self-consistent as possible, we perform calculations in the framework of nuclear DFT, which combines the Hartree-Fock-Bogoliubov (HFB) mean-field approximation to the energy with a many-body method inspired by Kohn-Sham density functional theory (DFT). An overview of the self-consistent framework is described below, followed by explanations of each of the dynamical calculations which we use to calculate fission properties.

2.1 Nuclear Density Functional Theory

Since nuclei are quantum mechanical systems, they can in principle be described using the Schrodinger equation. However, in practice one finds this type of description difficult or impossible, for two reasons:

- In order to use the Schrodinger equation, one needs to know how to describe the interaction between particles, such as between protons and neutrons. However, protons and neutrons are made up of quarks and gluons, which interact via the strong nuclear force. Consequently, an analytic expression for the nucleon-nucleon interaction analogous to the $\frac{1}{r}$ form of the Coulomb interaction is not available. Finding different mathematical expressions which can describe the interaction between nucleons continues to be an active area of research [?]
- Even when an interaction is known, nuclei are large systems made up of many protons and neutrons. Solving the Schrodinger equation directly quickly becomes computationally intractable as the number of nucleons increases.

2.1.1 Density Functional Theory

Kohn-Sham DFT is based on the Hohenberg-Kohn theorems

Let us define the nucleon density in the following way: suppose we have a system described in second quantization by a set of creation and annihilation operators c_i, c_i^\dagger which act on the [Fock-space?] vacuum state $|\psi_0\rangle$. The first Kohn-Sham theorem says that the energy of the system is a uniquely-defined functional of the density. That means that if a system of interacting particles and a system of noninteracting particles give the same density, the energy of those systems will be the same. This gives us the freedom to try to describe our system using a mean-field method instead of having to describe the pairwise interactions between every particle in the system - a huge simplification to the problem!

The second Kohn-Sham theorem states that the functional which gives the energy of the system will give the ground state energy if, and only if, it acts on the true ground state

density. Thus, given a particular functional, we can vary the input density to minimize the total energy and be assured that we are approaching the ground state energy of the system.

Suppose you have the density $\rho(\mathbf{r})$ of an interacting system of particles. There exists a unique noninteracting system with the same density. Then I believe HFB is put on top of that to do the variation part. I think I (approximately) get it now! - So just to make sure, what would DFT look like without HF/HFB? And HF/HFB without DFT?

Rather than find the density of a system of interacting particles (which can be extremely complicated - as one particle moves, the force it exerts on neighboring particles causes them to move, which will in turn change the magnitude and direction of the net force acting on the original particle, and so on until an equilibrium configuration, if it exists, can be attained), Kohn-Sham allows us to find an equivalent density of fictional non-interacting particles. That is, instead of particles moving in a field generated by many interdependent neighboring particles, one may think of non-interacting particles moving about a mean-field, which is essentially an averaging over all other particles.

Together, the Hohenberg-Kohn theorems state that if one is able to find the true ground state density, regardless of where it comes from, then there exists a unique functional of the density which gives the ground state energy of the system. However, HK do not specify how this functional is to be obtained.

For a variety of reasons/complications (refs 73-78 of [43]), pure Kohn-Sham is not used in nuclear physics; however, in the spirit, we oftentimes switch to a representation involving densities (which are directly and exactly attainable from a many-body wavefunction) and energy density functionals (which are not known exactly). (Wait, but then what is the point of converting to densities? Why not just leave them as wavefunctions? Or maybe we do, but this representation just makes the math look nicer for papers)

The basic idea is to replace the single particle states $c_i^\dagger |\psi_0\rangle$ with the single-particle density, $\rho_{ij} = \langle \psi_0 | c_j^\dagger c_i | \psi_0 \rangle$

Because pairing interactions are of great importance to nuclear dynamics, we also construct an additional density $\kappa_{ij} = \langle \psi_0 | c_j c_i | \psi_0 \rangle$, which can be thought of as a coupling between the vacuum state and a state with two particles (in states i and j). Together with the single-particle density ρ we construct a generalized density

$$\mathcal{R} = \begin{pmatrix} \rho & \kappa \\ -\kappa^* & 1 - \rho^* \end{pmatrix} \quad (2.1)$$

In coordinate space, the density matrix ρ and the pair tensor κ take the form

$$\rho(\vec{r}, \vec{r}') = \langle \psi_0 | c_{\vec{r}'}^\dagger c_{\vec{r}} | \psi_0 \rangle \quad (2.2)$$

$$\kappa(\vec{r}, \vec{r}') = \langle \psi_0 | c_{\vec{r}'} c_{\vec{r}} | \psi_0 \rangle \quad (2.3)$$

Recall that in nuclei, there is a ρ_n describing neutrons and a ρ_p for protons.

The total energy is a sum of several contributions:

$$E(\rho, \kappa) = E_{kin} + E_{Coul} + E_{nuc} + E_{pair} \quad (2.4)$$

where E_{kin} is the kinetic energy term, E_{Coul} contains the Coulomb interaction between protons, E_{nuc} is a phenomenological nucleon-nucleon interaction term, and E_{pair} describes the tendency of nucleons to form pairs, which is smeared out in non-interacting mean-field models. Finding a good nucleon-nucleon interaction E_{nuc} (and to a lesser extent, E_{pair}) to be used in calculations is an active topic of research in nuclear theory today (for one recent

example, see [26]); two types of interactions which are commonly-used today are the Skyrme and Gogny families of interactions \cite{???}. We use primarily Skyrme-type interactions, which are described below.

2.1.1.1 Kinetic term

Defining the kinetic density $\tau_\alpha = \nabla \cdot \nabla' \rho_\alpha(\vec{r}, \vec{r}')|_{\vec{r}=\vec{r}'}$, the kinetic energy contribution is

$$E_{kin} = \frac{\hbar^2}{2m} \left(1 - \frac{1}{A}\right) \int d^3\vec{r} (\tau_n(\vec{r}) + \tau_p(\vec{r})) \quad (2.5)$$

The $\left(1 - \frac{1}{A}\right)$ term is a simple, approximate center-of-mass correction.

2.1.1.2 Coulomb interaction

The Coulomb interaction between protons is divided into a direct term and an exchange term, which is related to the Pauli exclusion principle.

$$E_{Coul} = E_{Coul,dir} + E_{Coul,exch} \quad (2.6)$$

$$E_{Coul,dir} = \frac{e^2}{2} \int d^3\vec{r}_1 d^3\vec{r}_2 \frac{\rho_p(\vec{r}_1)\rho_p(\vec{r}_2)}{|\vec{r}_1 - \vec{r}_2|} \quad (2.7)$$

$$E_{Coul,exch} = \frac{e^2}{2} \int d^3\vec{r}_1 d^3\vec{r}_2 \frac{\rho_p(\vec{r}_2, \vec{r}_1)\rho_p(\vec{r}_1, \vec{r}_2)}{|\vec{r}_1 - \vec{r}_2|} \quad (2.8)$$

Often the exchange term is computed in the Slater approximation \cite[refs 27,28 of HF0DD-I]:

$$E_{Coul,exch} \approx -\frac{3e^2}{4} \left(\frac{3}{\pi}\right)^{\frac{1}{3}} \int d^3\vec{r} \rho_p^{\frac{4}{3}}(\vec{r}) \quad (2.9)$$

2.1.1.3 Skyrme interaction

The total Skyrme interaction energy density is a sum of both time-even and time-odd terms:

$$E_{Skyrme} = \int d^3\vec{r} \sum_{t=0,1} \left(\mathcal{H}_t^{even} + \mathcal{H}_t^{odd} \right) \quad (2.10)$$

$$\mathcal{H}_t^{even} = C_t^\rho \rho_t^2 + C_t^{\Delta\rho} \rho_t \Delta \rho_t + C_t^\tau \rho_t \tau_t + C_t^J \mathbf{J}_t^2 + C_t^{\nabla J} \rho_t \nabla \cdot \vec{J}_t \quad (2.11)$$

$$\mathcal{H}_t^{odd} = C_t^s \vec{s}_t^2 + C_t^{\Delta s} \vec{s}_t \Delta \vec{s}_t + C_t^T \vec{s}_t \cdot \vec{T}_t + C_t^j \mathbf{j}_t^2 + C_t^{\nabla j} \vec{s}_t \cdot (\nabla \times \vec{j}_t) \quad (2.12)$$

where τ_t is the kinetic energy density; \mathbf{J}_t is the spin current density, with vector part given by $\vec{J}_{\kappa,t} = \sum_{\mu\nu} \epsilon_{\mu\nu\kappa} \mathbf{J}_{\mu\nu,t}$; \vec{s}_t is the spin density, \vec{T}_t is the spin kinetic density; and \vec{j}_t is the momentum density (to see how these are related to ρ , see, e.g., [8]). The index $t = 0(1)$ refers to isoscalar(isovector) energy densities, e.g., $\rho_0 = \rho_n + \rho_p$ ($\rho_1 = \rho_n - \rho_p$). Note that \mathcal{H}_t^{even} depends only on time-even densities (and likewise for \mathcal{H}_t^{odd}).

Since this interaction is phenomenological, based on a zero-range contact interaction between nucleons, the coefficients are adjustable. There are dozens of Skyrme parameterizations on the market, each one optimized to a particular observable or set of observables. The parameter sets SkM* [7] and UNEDF1 [20] (along with its sister, UNEDF1_{HFB} [42]) are optimized to datasets which include deformed nuclei, making them suitable for fission.

2.1.1.4 Pairing interaction

We use a density-dependent pairing interaction:

$$E_{pair} = V_0 \int d^3\vec{r} \left(1 - \left(\frac{\rho(\vec{r})}{\rho_0} \right)^\alpha \right) \quad (2.13)$$

As with the nuclear interaction term, the pairing interaction contains several adjustable parameters.

2.1.2 Bogoliubov transformation

In anticipation of the HFB formalism below, we define the so-called Bogoliubov transformation. The fundamental entity in the Bogoliubov transformed basis are ‘quasiparticle’ states, defined by quasiparticle creation and annihilation operators acting on a quasiparticle vacuum state $|\Phi_0\rangle$ (in contrast to the single particle operators from before). The creation and annihilation operators are given by

$$\beta_\mu = \sum_i U_{i\mu}^* c_i + \sum_i V_{i\mu}^* c_i^\dagger \quad (2.14)$$

$$\beta_\mu^\dagger = \sum_i U_{i\mu} c_i^\dagger + \sum_i V_{i\mu} c_i \quad (2.15)$$

or in block matrix notation,

$$\begin{pmatrix} \beta \\ \beta^\dagger \end{pmatrix} = \begin{pmatrix} U^\dagger & V^\dagger \\ V^T & U^T \end{pmatrix} \begin{pmatrix} c \\ c^\dagger \end{pmatrix} \equiv \mathcal{W}^\dagger \begin{pmatrix} c \\ c^\dagger \end{pmatrix} \quad (2.16)$$

where the transformation matrix \mathcal{W} must be unitary to ensure that β, β^\dagger obey the fermion commutation relations [35]. In this transformed basis, the density matrix takes the form

$$\mathbf{R} = \mathcal{W}^\dagger \mathcal{R} \mathcal{W} = \begin{pmatrix} \langle \Phi_0 | \beta_\mu^\dagger \beta_\nu | \Phi_0 \rangle & \langle \Phi_0 | \beta_\mu \beta_\nu | \Phi_0 \rangle \\ \langle \Phi_0 | \beta_\mu^\dagger \beta_\nu^\dagger | \Phi_0 \rangle & \langle \Phi_0 | \beta_\mu \beta_\nu^\dagger | \Phi_0 \rangle \end{pmatrix} = \begin{pmatrix} 0 & 0 \\ 0 & I_N \end{pmatrix} \quad (2.17)$$

2.1.3 Hartree-Fock-Bogoliubov Equations

The ground state configuration of the system described by this particular energy density functional E is described by the density which minimizes $E(\mathcal{R})$. We can find this solution through the variational principle. We minimize the energy with respect to the generalized density, subject to the constraint that $\mathcal{R}^2 = \mathcal{R}$, or in other words, that the state remains a quasiparticle vacuum. Defining the HFB Hamiltonian $\mathcal{H}_{ba} \equiv 2\partial E/\partial \mathcal{R}_{ab}$, this variation leads to the result $[\mathcal{H}, \mathcal{R}] = 0$, which is called the Hartree-Fock-Bogoliubov equation. It is not typically solved in this form, but it can be recast into something more useful. Recalling that two Hermitian operators whose commutator is zero can be simultaneously diagonalized, we choose to diagonalize \mathcal{H} using the same Bogoliubov transformation W which diagonalizes \mathcal{R} :

$$W^\dagger \mathcal{H} W \equiv \mathcal{E} \quad \text{or} \quad \mathcal{H} W = W \mathcal{E} \quad (2.18)$$

where

$$\mathcal{E} = \begin{pmatrix} E_\mu & 0 \\ 0 & -E_\mu \end{pmatrix} \quad (2.19)$$

is a matrix of quasiparticle energies. In this form, the problem can then be solved iteratively: an initial density ansatz is chosen in order to construct the Hamiltonian density \mathcal{H} , after which the eigenvalue problem is solved, leading to new densities (since the densities are related to \mathcal{W}), which in turn leads to an updated \mathcal{H} . This procedure can be repeated indefinitely, until some predetermined convergence criterion is met.

Very often we will want to minimize the energy with the system subject to a particular

constraint. In that case we would replace the Hamiltonian E with the Routhian E' before variation. Typically E' introduces the constraints via the method of Lagrange multipliers. Some common examples might be this simple form of particle number restoration (more sophisticated forms, such as Lipkin-Nogami \cite{???}, also exist)

$$E' = E - \lambda_n \langle \hat{N}_n \rangle - \lambda_p \langle \hat{N}_p \rangle \quad (2.20)$$

where λ_α is determined later by the condition that $\langle \hat{N}_\alpha \rangle = N_\alpha$, or shape, where we might constrain a particular multipole moment (or set of multipole moments) to the value $\bar{Q}_{\lambda\mu}$

$$E' = E - \sum_{\lambda\mu} C_{\lambda\mu} \left(\langle \hat{Q}_{\lambda\mu} \rangle - \bar{Q}_{\lambda\mu} \right)^2 \quad (2.21)$$

2.1.4 Nucleon localization function

One of the tools we will be using quite a bit in this thesis is the nucleon localization function (NLF), introduced in [54]. The NLF is defined using the single particle density in the following way (with q =isospin and σ =spin/signature quantum number):

$$\mathcal{C}_{q\sigma} = \left[1 + \left(\frac{\tau_{q\sigma} \rho_{q\sigma} - \frac{1}{4} |\nabla \rho_{q\sigma}|^2 - \mathbf{j}_{q\sigma}^2}{\rho_{q\sigma} \tau_{q\sigma}^{TF}} \right)^2 \right] \quad (2.22)$$

where $\tau_{q\sigma}^{TF} = \frac{3}{5} (6\pi^2)^{\frac{2}{3}} \rho_{q\sigma}^{\frac{5}{3}}$. A localization value $\mathcal{C} \approx 1$ means that nucleons are well-localized; that is, the probability of finding two nucleons of equal spin and isospin at the same location in space is low. A value of $\mathcal{C} = \frac{1}{2}$ corresponds to a Fermi gas of nucleons, as found in nuclear matter.

The NLF offers greater insight into the underlying shell structure of the system than,

for instance, the single particle density. In particular, when applied to fission as in [40], it sometimes enables one to see the formation of well-defined prefragments whose shell structure is responsible for the peak of the fragment distribution.

2.2 Microscopic Description of Nuclear Fission

With the nuclear physics somewhat under control, we now move onto the problem of using it to describe fission. Recently in [39], an approach based on this assumption was used to compute fragment yields from a potential energy surface (PES) that was computed self-consistently, using the WKB approximation to describe the tunneling and Langevin dynamics to describe post-scission dissipation. The half-life can be computed as in [38].

2.2.1 Potential Energy Surfaces

In the adiabatic approximation, the primary degrees of freedom are nuclear shapes, and therefore the basic ingredient to fission calculations is a potential energy surface (PES). In principle, one could describe any three-dimensional shape using an infinite basis such as the multipole expansion which is often encountered in electrodynamics; however, for practical computations one must use a truncated set of only a few multipole moments (or, more generally, collective coordinates). Thus, an important challenge for researchers is to select the most relevant collective coordinates, ideally while demonstrating that others can be safely neglected.

Once the appropriate shape constraints are chosen, the PES is computed as a mesh: one DFT calculation per grid point. The value at each point is the HFB energy computed above, $E'(\vec{q})$.

2.2.2 Collective inertia

Just as important to the fission dynamics as the energy of the system is the collective inertia, which describes the tendency of the system to resist configuration changes (such as shape changes). The form of the collective inertia we use is the non-perturbative adiabatic time-dependent HFB (ATDHFB) inertia with cranking [6], which takes the form

$$M_{\mu\nu} = \frac{\hbar^2}{2} \frac{1}{(E_a + E_b)} \left(\frac{\partial \mathcal{R}_{(0),ab}^{21}}{\partial q_\mu} \frac{\partial \mathcal{R}_{(0),ba}^{12}}{\partial q_\nu} + \frac{\partial \mathcal{R}_{(0),ab}^{12}}{\partial q_\mu} \frac{\partial \mathcal{R}_{(0),ba}^{21}}{\partial q_\nu} \right) \quad (2.23)$$

The subscripts and superscripts are explained in the full temperature-dependent derivation of the collective inertia found in Appendix ???, but the important feature to note is that computing the inertia requires differentiating the density matrix with respect to a set of collective coordinates.

A perturbative expression for the ATDHFB inertia also exists, which allows one to estimate the inertia without taking derivatives of the density. It is computationally much faster and easier to implement, but it is less accurate and loses many of the important features of the inertia, as we shall see in Chapter ??? (294Og). Nevertheless, it is commonly-used in calculations and we shall use it later on.

Another common expression for the collective inertia comes from the Generator Coordinate Method (GCM). The GCM inertia also exists in two varieties: perturbative and non-perturbative [17]. Like the ATDHFB inertia, the perturbative GCM inertia is smoothed-out compared to the non-perturbative inertia. Both the perturbative and non-perturbative GCM inertias are found to be smaller in magnitude than their ATDHFB counterparts.

2.2.3 WKB Approximation

Spontaneous nuclear fission is a type of quantum tunneling; consequently, it should be described using quantum mechanics. If the wavefunction corresponding to the fissioning nucleus is assumed to be slowly-varying inside the potential barrier (which is the case under the adiabatic assumption), then the WKB approximation allows us to estimate the tunneling probability through a classically-forbidden region in the PES.

Consider a set of collective coordinates $\mathbf{q} \equiv (q_1, \dots, q_N)$. The most-probable tunneling path $L(s)|_{s_{\text{in}}}^{s_{\text{out}}}$ in the collective space is found via minimization of the collective action

$$S(L) = \frac{1}{\hbar} \int_{s_{\text{in}}}^{s_{\text{out}}} \sqrt{2\mathcal{M}(s)(V(s) - E_0)} ds, \quad (2.24)$$

where s is the curvilinear coordinate along the path L , $\mathcal{M}(s)$ is the collective inertia given by [38]

$$\mathcal{M}(s) = \sum_{\mu\nu} M_{\mu\nu} \frac{dq_\mu}{ds} \frac{dq_\nu}{ds} \quad (2.25)$$

and $V(s)$ is the potential energy along $L(s)$. E_0 stands for the collective ground-state energy. The dynamic programming method [5] is employed to determine the path $L(s)$. The calculation is repeated for different outer turning points, and each of these points is then assigned an exit probability $P(s_{\text{out}}) = [1 + \exp\{(2s)\}]^{-1}$ [4].

The half-life corresponds to the minimum action pathway, and the expression for the half-life is $T_{1/2} = \ln(2)/nP(s_{\text{min}})$. The parameter n is the number of assaults on the fission barrier per unit time and the standard value is $n = 10^{20.38} s^{-1}$.

2.2.4 Langevin Dynamics

After emerging from the classically-forbidden region of the PES, fission trajectories begin from the outer turning line and then evolve along the PES according to the Langevin equations:

$$\frac{dp_i}{dt} = -\frac{p_j p_k}{2} \frac{\partial}{\partial q_i} \left(\mathcal{M}^{-1} \right)_{jk} - \frac{\partial V}{\partial q_i} - \eta_{ij} \left(\mathcal{M}^{-1} \right)_{jk} p_k + g_{ij} \Gamma_j(t), \quad (2.26)$$

$$\frac{dq_i}{dt} = \left(\mathcal{M}^{-1} \right)_{ij} p_j, \quad (2.27)$$

where p_i is the collective momentum conjugate to q_i . The dissipation tensor η_{ij} is related to the random force strength g_{ij} via the fluctuation-dissipation theorem, and $\Gamma_j(t)$ is a Gaussian-distributed, time-dependent stochastic variable.

The fluctuation-dissipation theorem is given by the expression $\sum_k g_{ik} g_{jk} = \eta_{ij} k_B T$. It effectively couples the collective and intrinsic via the system temperature, given by $k_B T = \sqrt{E^*/a}$ where $a = A/10 \text{MeV}^{-1}$ parameterizes the level density and the excitation energy $E^* = V(s_{out}) - V(\mathbf{x}) - \frac{1}{2} \sum \left(\mathcal{M}^{-1} \right)_{ij} p_i p_j$.

Dissipation is treated in our work as a parameter, as a self-consistent description of dissipation is not yet known. However, work along this line has been started (maybe?) in refs 291-293 of [?] (see section 4.1.1 for the context). In the meantime, we use the values from [39] (Is this too specific for a thesis? You're not worried about the little numerical details, right? Just the big-picture ideas?)

Chapter 3

Two fission modes in ^{178}Pt

3.1 Asymmetric fission in the region of ^{180}Hg

As mentioned in the introduction, fission is most well-studied in the region of the actinides ($Z=90$ to $Z=103$), as many naturally-occurring isotopes in this region are fissile. Within this region, there is a characteristic tendency for fission fragment yields to be asymmetric (that is, one light fragment and one heavy fragment), with the heavy peak centered around $A \approx 140$. This has been understood as a manifestation of nuclear shell structure in the prefragments: doubly-magic ^{132}Sn drives the nucleus towards scission, and once the neck nucleons are divided up between the two fragments, we end up with the heavy fragment $A=140$ peak. As one moves to the lower- Z actinides, however, this tendency becomes less and less pronounced as yields tend to become more symmetric. Below thorium, it was generally believed until recently (though mostly not tested) that yields would continue to be symmetric as there was no doubly-magic nucleus candidate that could drive the system toward asymmetry as there is with actinides.

However, it was reported in a 2010 study [1] that neutron-deficient ^{180}Tl undergoes beta-delayed fission, leading to intermediate state $^{180}_{80}\text{Hg}_{100}$ which then decays into two fragments of unequal mass. This finding triggered a flurry of theoretical papers hoping to describe this new and unexpected phenomenon (for instance, see \cite{some papers}). A follow-up

study using ^{178}Tl [21] further established this as a region of asymmetric fission, and not just a one-time occurrence. Since then, other nuclei in the region have been studied, for instance using Coulex-induced fission reactions and compound nucleus (prompt?) fusion-fission reactions, and the finding is the same.

Nuclei in this region have a number of unique features which make them interesting for study, even aside from the unexpected fragment asymmetry. Predicted fission barrier heights in this region are relatively-low (of the order of 12 MeV), making them suitable for study using low-energy techniques such as β -delayed fission (maybe [2] and the work at ISOLDE at CERN?) or Coulex-induced fission (maybe [22] and the SOFIA (Studies On Fission with Aladin) experiment/project/campaign). On the other hand, it has been found that compound nuclei formed in this region from particle-induced reactions tend to have high excitation energies, even for beam energies near the Coulomb barrier. This combination makes the region particularly well-suited for studies involving a variety of excitation energies.

Later experiments performed with isotopes in this region at different excitation energies have shown that, unlike the case of actinides where shell structure and fragment asymmetry is “washed out” at high excitation energies, mass asymmetric fragment distributions are a persistent feature of this mass region for various excitation energies. (A lot of good citations for this section can come from section 4.1.1 of [3]) An up-to-date (as of around 2016) overview of nuclei in the region of $^{180}_{80}\text{Hg}_{100}$ which have since been experimentally studied, including the experimental technique used, is shown in Figure 3.1.

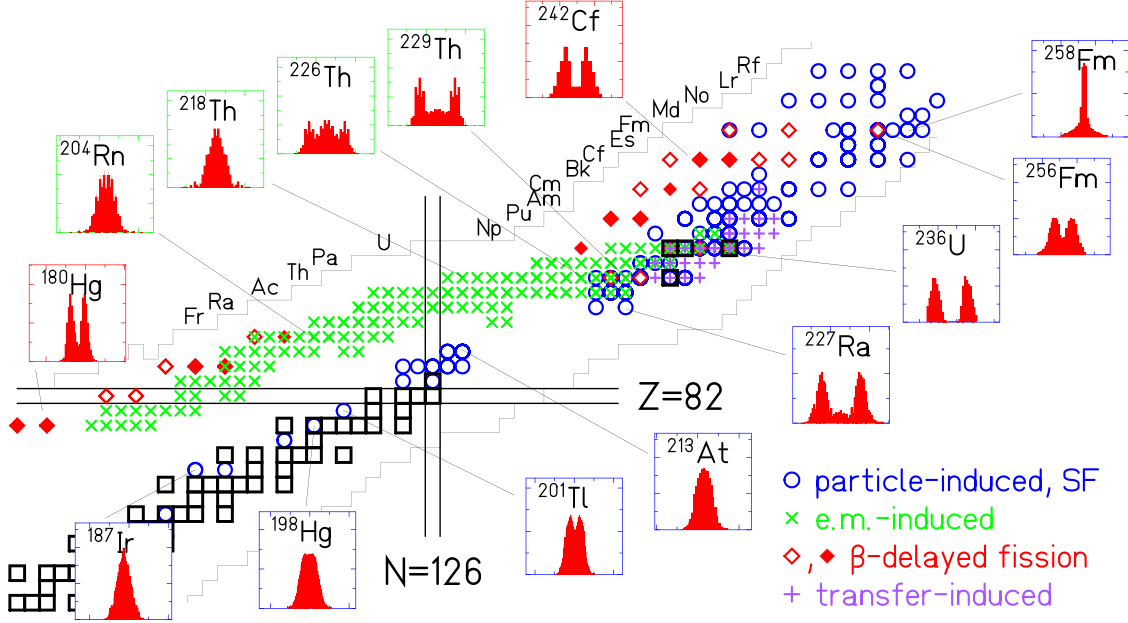


Figure 3.1: Fragment yields for several nuclei ranging from actinides, where primary fission yields tend to be asymmetric, down to near-thorium, where yields become more symmetric except in the region near neutron deficient $^{180}_{80}\text{Hg}_{100}$. Figure from [3].

3.2 Multimode fission of ^{178}Pt

One particular follow-up experiment was performed investigating spontaneous fission of $^{178}_{78}\text{Pt}_{100}$ [?], which differs from $^{180}_{80}\text{Hg}_{100}$ by 2 protons. This system was studied at various excitation energies and found to fission consistently with a bimodal pattern, as shown in Figure 3.2. Of the nuclei which underwent spontaneous fission, roughly 1/3 were found to fission symmetrically while the other 2/3 fissioned asymmetrically with a light-to-heavy mass ratio of approximately 79/99. Furthermore, it was observed that symmetric fragments tended to have higher kinetic energies than non-symmetric fragments.

To better interpret the results of this experiment, DFT calculations were performed using the functionals UNEDF1_{HFB} [42] and D1S [9]. These calculations involved computing a PES using the collective coordinates Q_{20} and Q_{30} . [Do I need to describe the calculations in detail here, or should I refer to the published papers (e.g. “Details of the calculation are given in

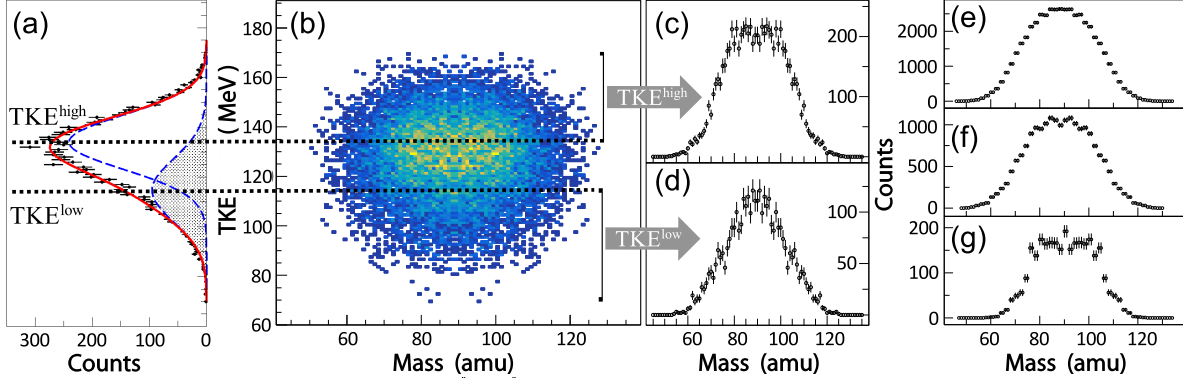


Figure 3.2: This figure contains the data from the $^{178}\text{Pt}_{100}$ experiment. I should go through and describe what all the individual boxes are for. Then I should cite out paper, once it's citeable

the paper”)?]

The UNEDF1_{HFB} PES is shown in Figure 3.3, while the D1S PES is in Figure 3.4. A calculation with full Langevin dynamics was not performed; however, the static (minimum-energy) pathway shown in the figure corresponds to a fragment split $A_L/A_H \approx 80/98$.

Also shown in Figure 3.3 are nucleon localization functions (recall Section) corresponding to various configurations in the PES. Along the symmetric path (ABcd in the figure), the fragments appear highly-elongated, with a rather large neck, even shortly before scission. Since elongation tends to minimize the Coulomb repulsion between fragments, then this configuration might be expected to lead to fragments with relatively low kinetic energies. On the other hand, compact fragments such as those in ABCD will tend to have a larger Coulomb repulsion, propelling the fragments away from one another with greater force and resulting in fragments with a higher kinetic energy. [We note that this is compatible with experiment]

Now consider the PES corresponding to the D1S functional in Figure 3.4. We note with some relief that, despite the inherent differences between the functionals, and despite the relative flatness of the surface with few discernible topological features, the overall topology

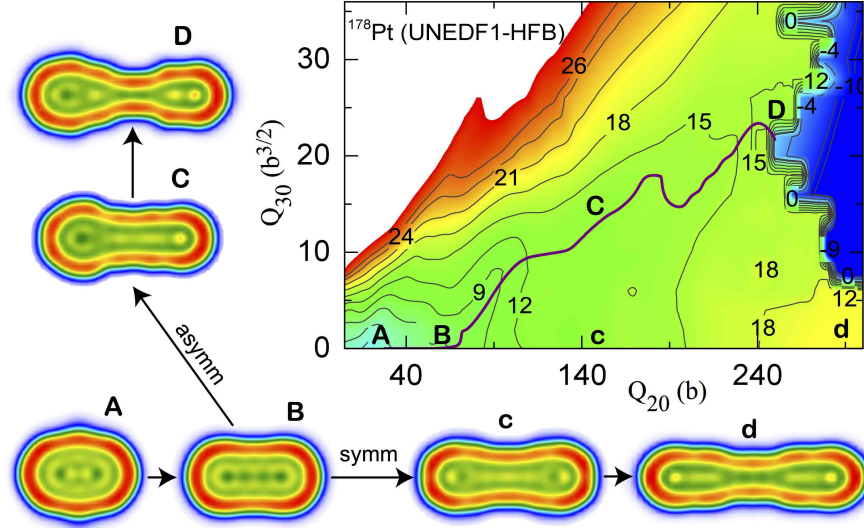


Figure 3.3: UNEDF1-HFB potential energy surface for ^{178}Pt . Note the two different trajectories ABCD and ABcd and their corresponding localizations.

of the PES is similar in both cases. The overall magnitude is different, but the static pathway follows a similar trajectory.

3.3 The physical origin of fragment asymmetry in the region of ^{180}Hg

Why is there a region of symmetric fission below thorium?

(These are notes from the 178Pt paper draft. Not mine, of course, but they have some good points to address): “Namely, the PES are predicted to be flat and much less structureless, and defined predominantly by the large liquid drop/macroscopic contribution, rather than by relatively small microscopic effects. Due to this, FFMDs exhibit fairly low dependence.. [refer to 180Hg PLB, as one example].

“(this was an answer by Witek, when somebody asked a question to my talk at Tsukuba - why the lead region is less sensitive to temperature.. the answer was - there is no ‘barrier’

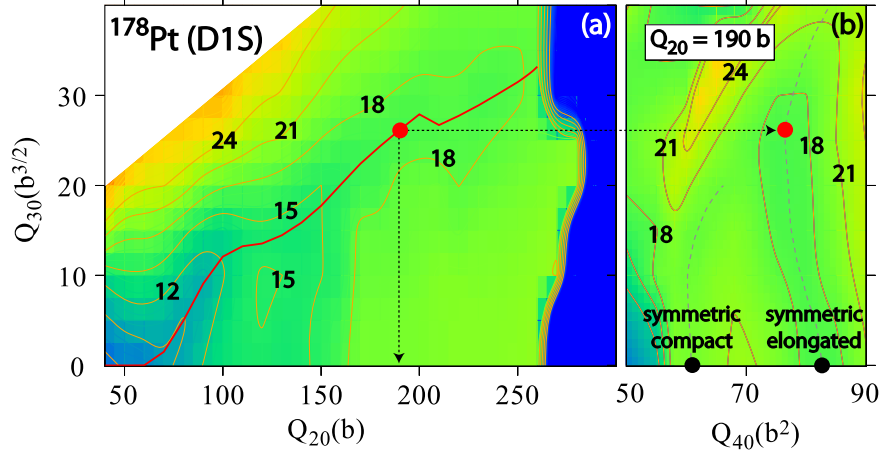


Figure 3.4: D1S potential energy surface for ^{178}Pt . Note also the additional information about the hexadecapole moment.

in a sennce, it's just flat/thick macroscopic surface, hardly influenced bu shell effects.. so, even if one heats it up, tiny shell effects will be gone, but the main underlying macroscopic part will remain).”

Peter Moller argues in the concluding discussion of (<https://link.aps.org/doi/10.1103/PhysRevC.85.024401>) [25]) that we can't really use the fragment/prefragment shell structure arguments in this region, and thus that we have yet to identify all the essential physics which determines fragments. He says the yields are given (at least in this case) by subtle interplays in local regions of the potential energy surface.

Witek, Michal Warda, and Staszczak argue in Section IV. *Prescission Configurations* of [49] that ^{180}Hg deforms as a molecular system consisting of ^{90}Zr and ^{72}Ge , with the remaining neck nucleons being distributed at scission to give the fragments they found in the experiment. Similarly, they make the same claim for ^{198}Hg , except using ^{98}Zr and ^{80}Ge . The first one kind of makes sense to me since ^{90}Zr is semi-magic, but ^{98}Zr is not and neither is ^{80}Ge . I wonder what might have happened had they tried to match up the densities of a different set of nearby nuclei (they used these because they had the same N/Z ratio as the

fissioning parent nucleus). Then in the conclusions: “We conclude that the mass distribution of fission fragments in both nuclei is governed by shell structure of pre-scission configurations associated with molecular structures.”

In the introduction to [23] it is stated as though conclusively that “the main factor determining the mass split in fission are shell effects at pre-scission configurations, i.e., between saddle and scission” (see also some additional references therein). I think the thing that is most selling it to me so far, though, is Fig. 3 from this paper, wherein they show the shell correction energy for each of the nuclei considered. Even though the PES itself is mostly flat in each of these cases, the magnitude of the shell correction is different whether you are looking at symmetric or asymmetric trajectories, and the one with the larger magnitude shell correction happens to be the one that wins out in the final fragment distribution. I’d also be curious to see what the collective inertia looks like, but this seems to at least give something. It’s not like this shell correction gets added on top of the PES - the PES is still relatively-flat - but it at least gives an explanation for why our traditional physical intuition is not totally failing us here.

Interesting future work in this region might include calculations with full dynamics (including from nuclei with excitation energy), as suggested in the conclusions of [23]

Chapter 4

Cluster decay in ^{294}Og

4.1 Cluster emission in Superheavy Elements

The region of superheavy elements ($Z > 104$) is an interesting one for the study of spontaneous fission because the liquid drop model predicts that all isotopes with $Z > 104$ are unstable with respect to spontaneous fission. These nuclei are stabilized due to shell effects, but they nevertheless remain short-lived and many of them will decay by spontaneous fission regardless.

Experimentally, spontaneous fission has been observed from several superheavy isotopes (see the right panel of Figure 4.1). Other observed SHEs undergo a series of alpha decays, which chains terminate in spontaneous fission. Furthermore, a variety of models predict regions of spontaneous fission in the superheavy regime. One example is shown in Figure 4.1, in which lifetimes were computed for several types of decays using empirical formulas and the results compared to estimate branching ratios. Figure 4.2 is similar, except that the spontaneous fission lifetimes were computed microscopically, as were the Q_α values used to estimate alpha decay lifetimes.

cluster emission [?, 27, 36]

From the theoretical point of view, half-life calculations based on semiempirical models predict cluster radioactivity to be the dominant decay channel of several superheavy nu-

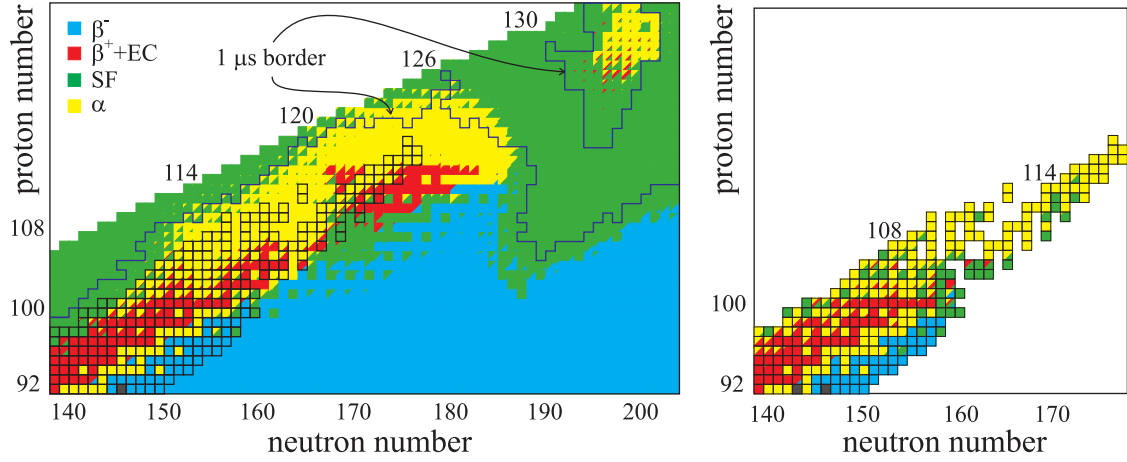


Figure 4.1: Calculated (left) and experimental (right) decay modes for SHE, based on an analysis of lifetimes calculated via empirical formulae. The boxed isotopes in the left panel are those which have been measured experimentally. Isotopes falling inside the $1\ \mu\text{s}$ contour are predicted to live longer than $1\ \mu\text{s}$. Figure adapted from [19].

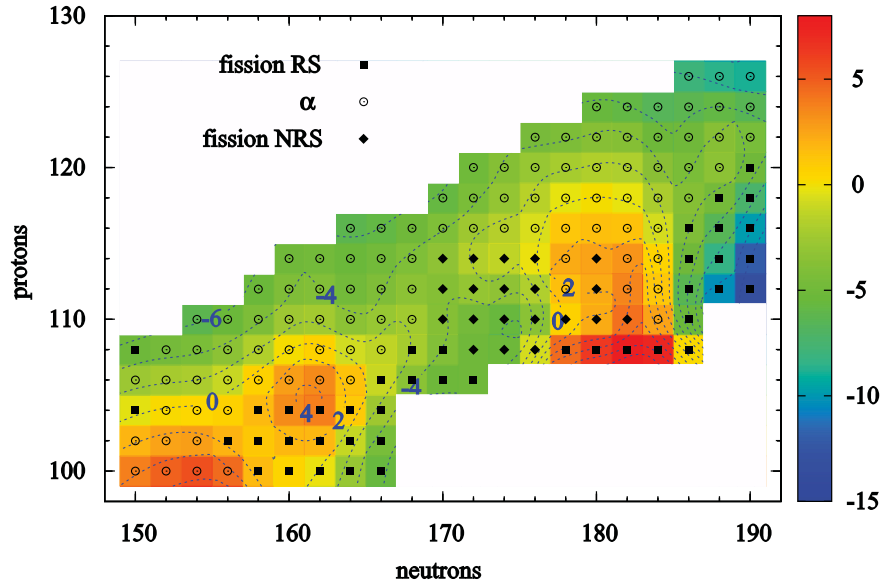


Figure 4.2: Dominant decay modes for SHE in a nuclear DFT-based framework are indicated. The label "RS" stands for "reflection symmetric" and "NRS" stands for "non-reflection symmetric." The colorbar indicates the predicted half-life on a logarithmic scale. Figure from [47].

clei [29, 30, 31, 32, 28, 41, 55]. Similar predictions have been obtained by more microscopic calculations using nuclear DFT framework [48, 50].

Poenaru and others have predicted in [29, 30, 31, 32, 28, 41, 55] that many superheavy elements will decay into two fragments, with the heavy fragment near the doubly-magic nucleus $^{208}_{82}\text{Pb}_{126}$. This particular decay mode is significant enough to have earned its own name in the literature, where it is known variously as cluster emission, cluster radioactivity, or lead radioactivity [?, 27, 36, 33]. The phenomenon of cluster emission was first observed in the decay $^{223}_{88}\text{Ra} \rightarrow ^{209}_{82}\text{Pb} + ^{14}_6$ [?] and has since been observed in several actinides. In all cases seen so far, it is a rare event with a small branching ratio [33].

The mechanism of cluster emission is based on the stability of the doubly-magic nucleus $^{208}_{82}\text{Pb}_{126}$. $^{294}_{118}\text{Og}_{176}$ is an excellent candidate for cluster emission because the cluster it is predicted to emit, $^{86}_{36}\text{Kr}_{50}$, receives additional stability due to its having a magic number of neutrons. Semiempirical arguments based on the symmetry energy lend additional support to this candidate, since $^{294}_{118}\text{Og}_{176}$ and $^{208}_{82}\text{Pb}_{126}$ have a similar N/Z ratio [50].

We took this prediction one step further than the aforementioned by calculating the full spontaneous fission fragment distribution of $^{294}_{118}\text{Og}_{176}$. As we will show, the distribution is sharply-peaked around $^{208}_{82}\text{Pb}_{126}$. Furthermore, the distribution is quite robust with respect to the inputs of the calculations. We will also visualize the formation of the fragments using the nucleon localization function.

4.2 Predicted spontaneous fission yields of ^{294}Og

We calculated the spontaneous fission fragment yields for $^{294}_{118}\text{Og}_{176}$ under a variety of conditions. First, we elected to using three distinct EDFs: UNEDF1_{HFB}[42], a Skyrme functional

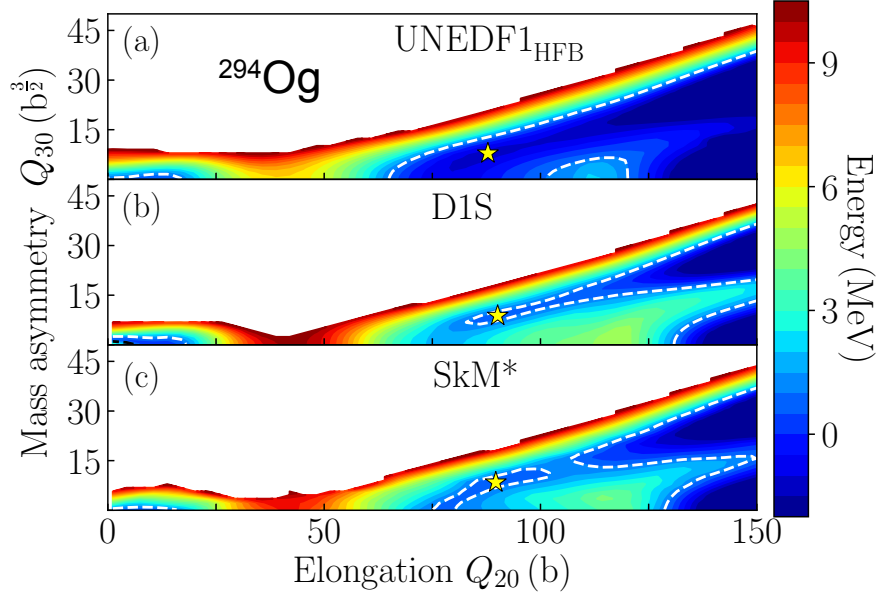


Figure 4.3: Comparison of the PESs for $^{294}_{118}\text{Og}_{176}$ in the (Q_{20}, Q_{30}) collective plane obtained in UNEDF1_{HFB} (a), D1S (b), and SkM* (c) EDFs. The ground-state energy E_{gs} is normalized to zero. The dotted line in each figure corresponds to $E_0 - E_{gs} = 1$ MeV, which was used to determine the inner and outer turning points. The local energy minima at large deformations are marked by stars.

which was optimized to data for spherical and deformed nuclei, including fission isomers; SkM* [7], another Skyrme functional designed for fission barriers and surface energy; and D1S [9], a parametrization of the finite-range Gogny interaction fitted on fission barriers of actinides. [I don't know whether to describe the calculations here (in which case I might as well just quote the original paper), or if I should just state that "Details of the calculation are shown in \cite{???}." or somewhere in between, where I still describe the collective space and the inertias, but maybe not the HFODD basis.]

We start by showing 2-dimensional projections of the calculated PESs in Figure 4.3.

The resulting distributions are shown in Figure 4.4.

As expected, the yields are peaked in the region of $^{208}_{82}\text{Pb}_{126}$ with a sharp fall-off. Likewise, we can see this by looking at the projections of the distributions onto the mass and charge shown in the top panels of Figure 4.5.

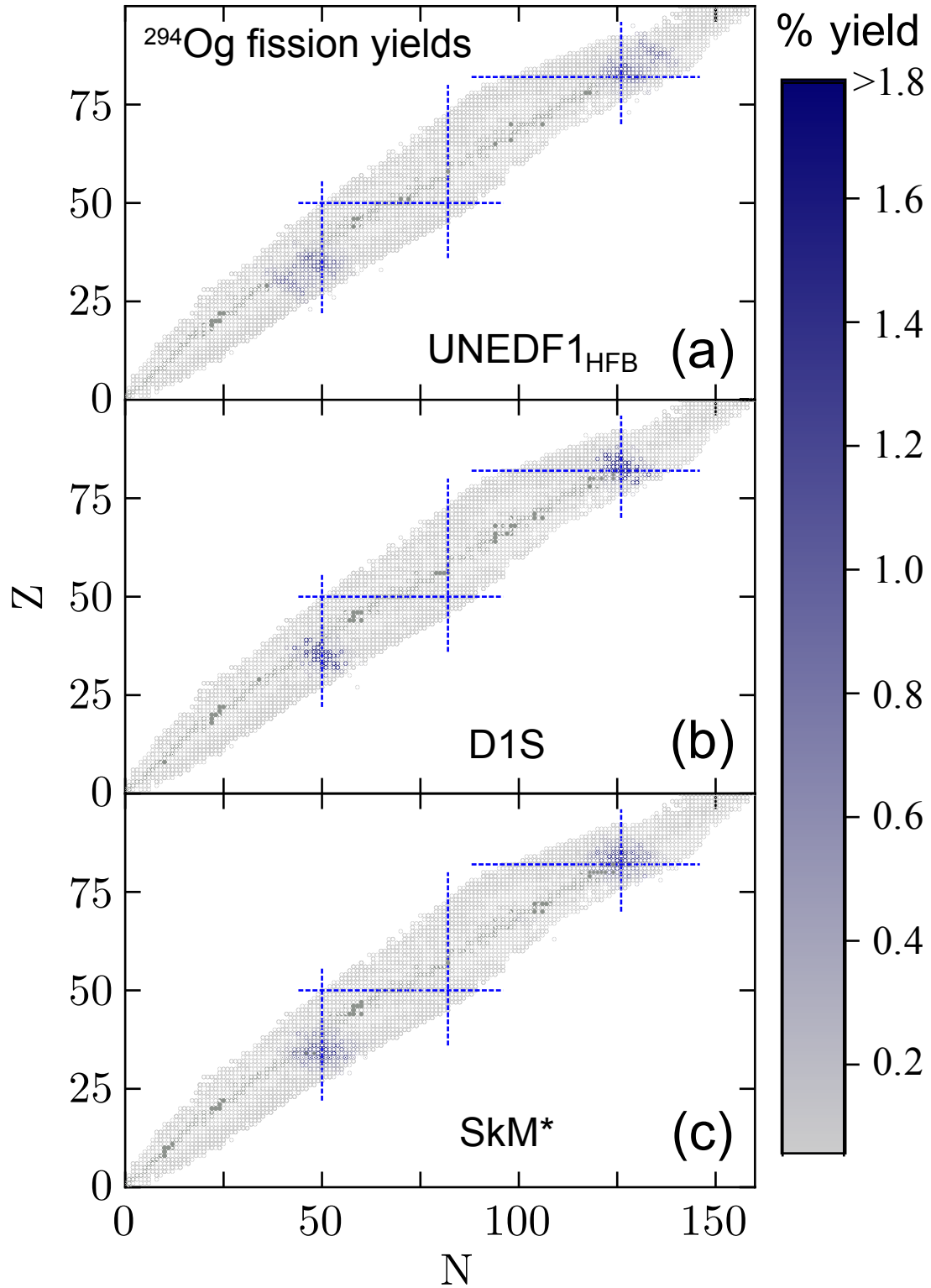


Figure 4.4: Fission fragment distributions for $^{294}_{118}\text{Og}_{176}$ obtained in UNEDF1_{HFB} (a), D1S (b), and SkM* (c) EDFs using the non-perturbative cranking ATDHFB inertia and the baseline dissipation tensor η_0 . Known isotopes are marked in grey [?]. Magic numbers 50, 82, and 126 are indicated by dotted lines.

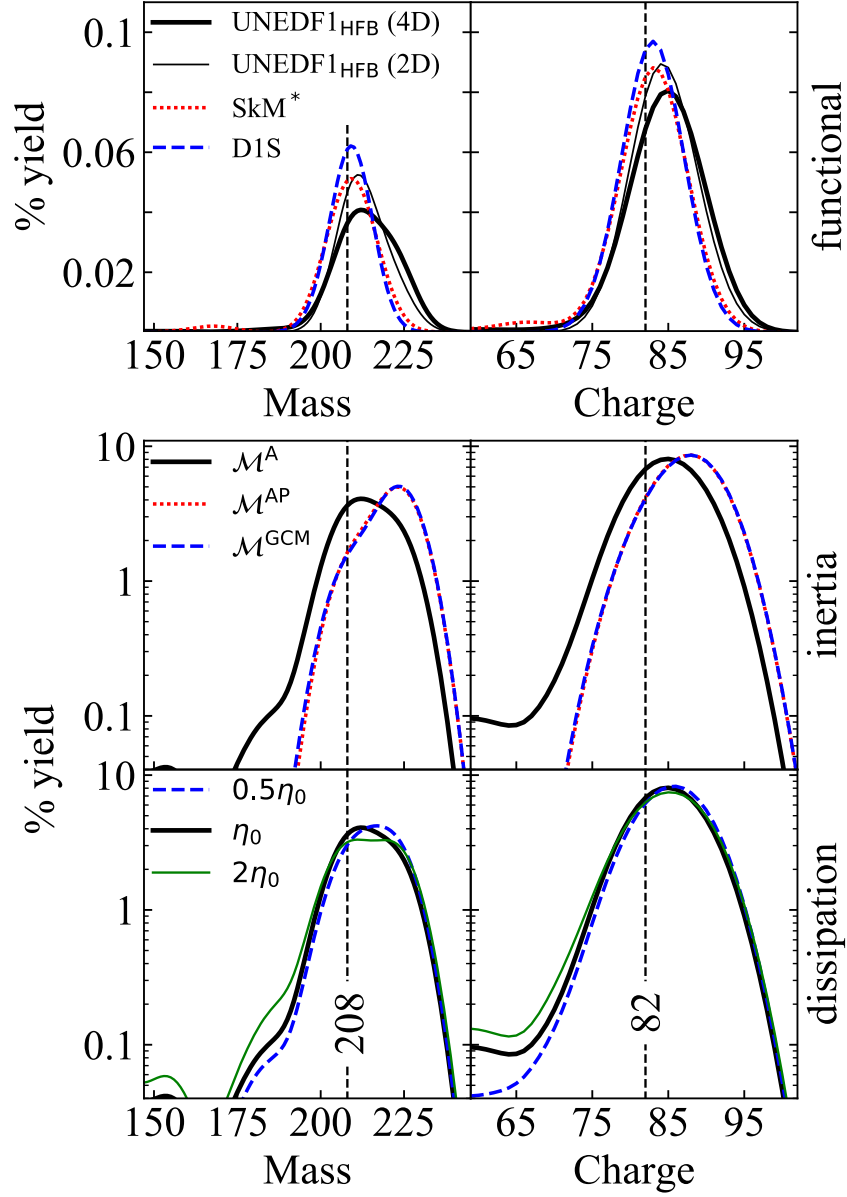


Figure 4.5: Upper panel: Predicted heavy fragment mass (left) and charge (right) yields of $^{294}_{118}\text{Og}_{176}$ using different functionals (top, linear scale). Bottom panels: collective inertias and dissipation tensor strengths (in logarithmic scale). The baseline calculation was performed using the UNEDF1_{HFB} functional in a 4D space with non-perturbative cranking ATDHFB inertia and dissipation tensor strength η_0 .

As discussed in the introduction, the collective inertia can also have a large impact on the fission dynamics. Using the UNEDF1_{HFB} functional, we compared our result with the non-perturbative cranking ATDHFB inertia \mathcal{M}^A to the perturbative ATDHFB \mathcal{M}^{AP} (which appears smoothed-out compared to \mathcal{M}^A) and perturbative GCM \mathcal{M}^{GCM} (which is smooth and also lower in magnitude than \mathcal{M}^A or \mathcal{M}^{AP} by roughly a factor of 1.5), which are often easier to use for large-scale calculations. The result, shown in the middle panels of Figure 4.5, show that the distribution has shifted slightly, but that \mathcal{M}^{AP} and \mathcal{M}^{GCM} give identical, or nearly-identical results. The smoothness of the perturbative inertias apparently allow fluctuations to drive the system to more extreme fragment configurations. This suggests that the magnitude of the inertia matters less than the topography for computing fission yields (though we note that this would not be true for calculating half-lives, which depend exponentially on the magnitude of the inertia).

We also vary the strength of fluctuations by adjusting the parameter η . Our starting point η_0 is taken from reference [39], where it was obtained by adjusting η to match the experimental fragment distribution of ^{294}Pu . Shown in the bottom panel of Figure 4.5, we find that fluctuations do not affect the peak of the distribution, consistent with the results of Refs. [34, 44, 40]. The primary effect is in the tails.

4.3 ^{294}Og

However, although various attempts have been made to demonstrate the validity of this assumption, our work represents the first published instance of a 4D potential energy surface calculated self-consistently. Furthermore, given the recent demonstration of the importance of pairing correlations as a collective “coordinate” of the system, ours will feature pairing as

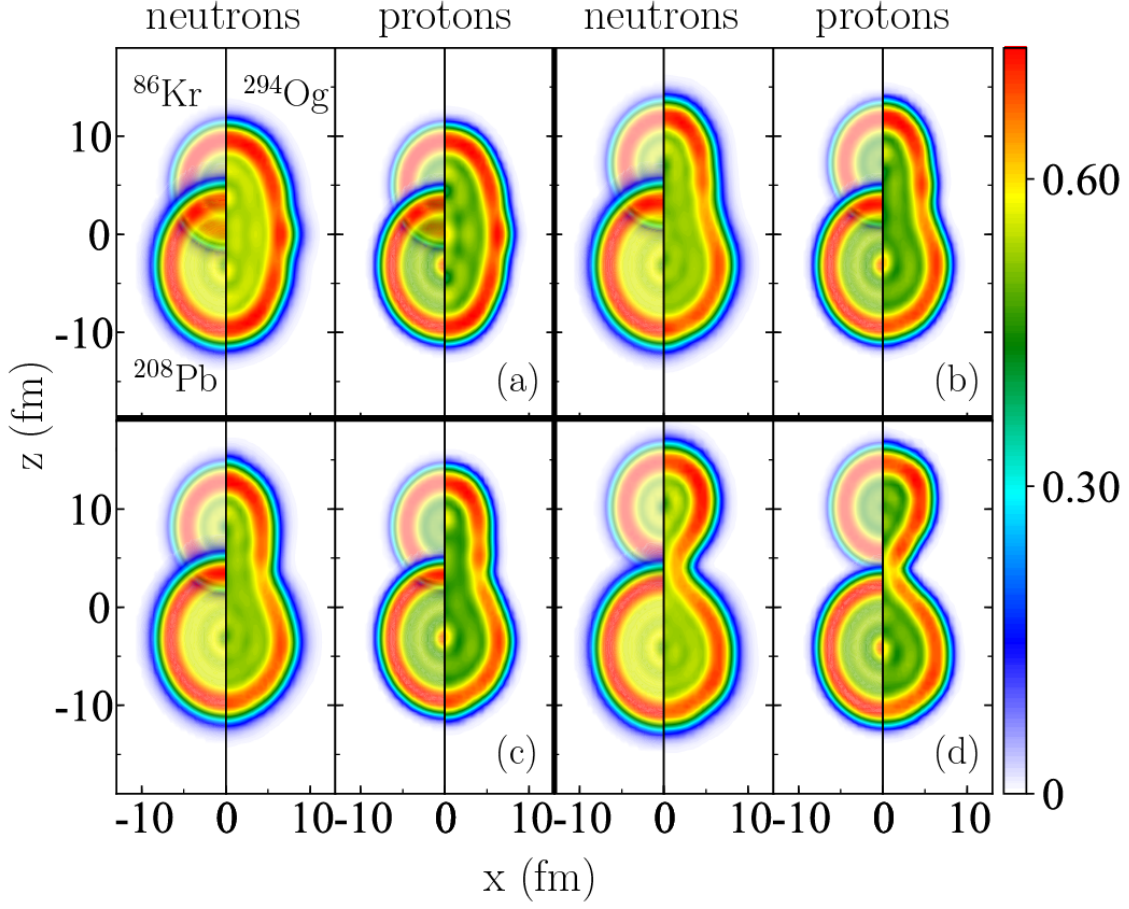


Figure 4.6: Nucleon localization functions for several deformed configurations of $^{294}_{118}\text{Og}_{176}$. For comparison, localizations are shown for the fragments $^{208}_{82}\text{Pb}_{126}$ and $^{86}_{36}\text{Kr}_{50}$ on the left side of each subplot. The configurations shown correspond to Fig. 1 from the paper, with multipole moments $(Q_{20}, Q_{30}) =$ (a) $(75 \text{ b}, 0)$; (b) $(120 \text{ b}, 17 \text{ b}^{\frac{3}{2}})$; (c) $(140 \text{ b}, 24 \text{ b}^{\frac{3}{2}})$; and (d) $(264 \text{ b}, 60 \text{ b}^{\frac{3}{2}})$.

part of the collective space, and its impact compared to other collective coordinates will be evaluated.

We used 30 harmonic oscillator shells and 1500 states

4.3.1 Cluster Decay

Experimental instances of super-asymmetric fission: M. G. Itkis 1985, Z Phys A 320 - no assessment of the cause of highly-asymmetric fission, but likely related to ^{132}Sn (these nuclei would tend to fission symmetrically, but with a slight bump around mass $A=140-145$) D. Rochmann Nucl Phys A 735 (2004) - driven by shell structure of lighter fragments I M Itkis, J Phys Conf Ser 515 (2014) 012008 - cluster radiation by another name

AKA “Lead Radioactivity” sometimes in the literature

4.3.2 Competition with Alpha Decay or Half-lives

[29, 30] - In this paper they propose changing/extending the concept of Heavy Particle Radioactivity or Cluster Radioactivity. Also they apply some model to HPR/CR in SHE.

4.4 Method

Our calculations were performed within the framework of nuclear density functional theory using Skyrme and Gogny energy density functionals. In the Skyrme case, the parameterization UNEDF1-HFB [42] was used, and pairing correlations were described using a density dependent pairing interaction. To assure convergence despite the high density of states, the DFT solver HFODD was used with 30 harmonic oscillator shells and 1500 states allowed in the calculation. Calculations were performed in a 4D collective space consisting of 3

shape coordinates, (q_{20}, q_{30}, q_{22}) , and, given the importance of dynamic pairing fluctuations demonstrated in [37], λ_2 . To demonstrate model independence, another set of calculations was performed using the Gogny energy density functional D1M in the two-dimensional collective space described by coordinates (q_{20}, q_{30}) .

It is seen in many models that introducing triaxiality as a degree of freedom can often be energetically-favorable, sometimes lowering saddle points by as much as 3 MeV; however, dynamic calculations in which the collective inertia is considered together with the potential energy surface have found that dynamical pathways usually tend to tunnel through barriers rather than break axial symmetry. This competition was explored for SHE in [16], with the conclusion that triaxiality plays a fairly insignificant role in determining the half-life of elements below $Z = 120$. However, another recent paper (<https://arxiv.org/abs/1803.04616v2>) suggests that triaxiality might significantly lower the second barrier. Regardless, we included q_{22} in our calculations. It may also be the case that isotopes which are oblate-deformed in their ground state may pass through triaxial configurations on their way to greater elongations.

4.5 Experimental efforts to find cluster emission in ^{294}Og

Perhaps the biggest uncertainty we'll see, or the biggest deviation from experiment, will be the distribution width. That's because we rather arbitrarily used $\sigma_A = 6, \sigma_Z = 4$. The values used in ^{240}Pu were 3 and 2, but the Q_N value they used was quite a bit smaller too. Since we had a much larger Q_N cutoff, we needed to account for larger particle number fluctuations. But these numbers were just kind of arbitrary. I'm not too worried about this because the peak is the part that matters, and we clearly saw a peak at the cluster location.

They found 3 (and possibly 4) instances in the original Dubna run. Another Og paper (Brewer2018) has a similar decay chain but a shorter half-life (~ 0.185 ms); Detected a 10.6 MeV recoil event, followed 78 microseconds later by a second decay event in the same pixel (~ 140 MeV), which is a candidate for SF.

[13] they've already started looking, and they're building a new detector that might be able to see it better.

Chapter 5

R-process

I'll say some stuff about r-process nuclei here

Fission inputs to r-process network calculations

You should definitely cite the 2015 paper by Eichler et al (doi:10.1088/0004-637X/808/1/30), titled “THE ROLE OF FISSION IN NEUTRON STAR MERGERS AND ITS IMPACT ON THE r-PROCESS PEAKS”. The region of largest variation (in their conclusions, at least) is in the region $A=100-160$, which makes sense because that's where most of your fission fragments are likely to lie. This is roughly-speaking also the region of that rare-earth peak everyone always talks about, along with the so-called second r-process peak.

Kilonova - the bright burst of gamma rays and other radiation that accompanies a compact object merger, presumably created mainly from the radioactive decay of unstable r-process nuclei (mainly via alpha and beta decay, but not fission - according to <https://www.nndc.bnl.gov/> see also the paper [56])

Light curves - show the magnitude/intensity of light/EM radiation as a function of time. For example, the light curve from the sun on the earth will be roughly sinusoidal; from an eclipse, you'll have a roughly straight line, then a dip, then a return to the original straight line; a pulsar will also be something regular and periodic. Each type of nova/supernova/kilonova/etc. has its own characteristic light curve, with an initial peak of varying sharpness, and then a gradual decay (though how gradual depends on the char-

acteristics of the event).

Heating - Is exactly what it sounds like. When a nucleus decays, it loses energy. Some of that energy escapes in the form of neutrinos or photons, while other energy is absorbed elsewhere in the medium. A related concept is opacity. Heavier nuclei with a large level density tend to be more opaque because they can more readily absorb photons than smaller, less opaque nuclei. And the process by which all of this energy exchange takes place is called thermalization.

The idea behind this $^{254}_{98}\text{Cf}_{156}$ calculation is related to [56]: There is some speculation that the heating from the NSM might be strongly-impacted by spontaneous fission of $^{254}_{98}\text{Cf}_{156}$. A related idea that $^{254}_{98}\text{Cf}_{156}$ may have been a large contributor to supernova (not kilonova) lightcurves dates back to 1956 (see references in Zhu’s introduction), but perhaps fell out of favor once it was discovered that the decay chain of ^{56}Ni was the primary contributor.

Mass and kinetic energy distributions of $^{254}_{98}\text{Cf}_{156}$ were actually measured in [12]. For some reason, though, Zhu considers that measurement “sparse” and they do some dressing up of it in their paper.

Since $^{254}_{98}\text{Cf}_{156}$ is heavier than actinides, detecting its presence in kilonovae would help solidify the location of r process nucleosynthesis. And if it has as large an impact on the heating and light curves as [56] says, it might well make the difference between “hard-to-observe” and “somewhat easier to observe.”

So what was it about the fission of $^{254}_{98}\text{Cf}_{156}$ that [56] needed in order to make this argument? And how did they zero-in on $^{254}_{98}\text{Cf}_{156}$ to begin with? These are good questions that nobody knows the answer to. Nah, I’m just kidding. The answer is out there. I just need to find it. It is one of a handful of isotopes which *could* be produced in significant amounts during an r process scenario and which is known to undergo spontaneous fission,

along with other californium and fermium isotopes. Furthermore, its half-life on the order of several days means that it could potentially make a significant impact on heating, especially at later times. The group of nuclei matching these criteria include $^{254}_{98}\text{Cf}_{156}$, ^{257}Es , and ^{260}Md . Finally, according to the mass model and branching ratios they used in [56], the other two nuclei seem like maybe they're more likely to β -decay, so $^{254}_{98}\text{Cf}_{156}$ it is. I talked to Samuel, and he says that everybody else predicts $^{254}_{98}\text{Cf}_{156}$, too.

Will you not also want/need to mention your work on ^{290}Fm ? This $^{254}_{98}\text{Cf}_{156}$ is not all that neutron rich, nor is it far from the region most-commonly studied. So perhaps you should say and do a bit more work on Fermium. Even just to say that triaxiality is not important here is something and not nothing. The reason you began to study this particular nucleus, though, is that based on Trevor Sprouse's r process network calculations (which utilized Peter Moller's fission calculations) and depending on the specifics of the astrophysical conditions, fission terminates the r process in a region of the N-Z plane. ^{290}Fm falls into the range identified in one of these calculations (it would be good to cite it) and was selected by Trevor as one which may be particularly significant. However, looking back over my emails, it seems like this is not a robust finding. Other predictions (like the ones I have from Samuel and Marius Eichler) seem to perhaps indicate that I'd be better off looking in the region for which ^{280}Fm is the northeast corner, perhaps.

Chapter 6

Fragment Identification

6.1 Fragments and the Nucleon Localization Function

An improved scission criterion would go beyond simply counting the number of particles in the neck. To help with this, we have a tool at our disposal which helps us to understand correlations that affect fission dynamics. This is called the nucleon localization function, and it allows us to visualize the prefragment nuclear shell structure which largely determines the identity of fission fragments [54].

The nucleon localization function shows that some prefragments can be very well-formed even when the neck is large, while in another case the neck might be small but the prefragments, poorly-defined [40]. A better scission criterion should take into account, or at least be compatible with, the insights gained from the nucleon localization function. As noted in [52], fragment properties on either side of the scission line may differ drastically. This is because shell structure is not well-described geometrically. Our localization measure offers an alternative scheme for identifying fragments before the scission line (see [40]). Since it is based on the underlying quantum shells, it is less sensitive to fluctuations and particle rearrangements late in the evolution.

6.2 The problem of scission

For practical reasons we are limited to describing complicated shapes in terms of just a few parameters, leading to uncertainty in the fragment properties. In particular, the part of the process at which the neck snaps and one nucleus becomes two, called scission, is not well-defined in static approaches.

Many times in static approaches, including the results shown in this dissertation so far, scission is frequently characterized by a single number such as Q_N , which approximately corresponds to the number of particles in the neck. When that number falls below a certain predefined threshold, we say that the nucleus has scissioned. Fragments are identified and one can try to estimate the strength of the repulsive interaction forcing the fragments apart. Of course, as discussed by Younes and Gogny in [?, 53], wavefunctions corresponding to individual nucleons may extend into the spatial region of the opposite fragment.

This can be understood with an analogy: suppose we stretch a nucleus until a neck forms, and then we use a butcher knife to lop the two fragments apart. This works reasonably well for estimating fragment mass and charge, but it is very poor when it comes to estimating the relative energy of the fragments. To estimate fragment kinetic and excitation energies, one needs to carefully and delicately peel the interlocking fragments apart with a scalpel, or a proper accounting of entanglement and other many-body correlations.

Essentially what we show is that Q_N is meaningless, and that any static definition of scission is going to need to account for the actual configuration of the system.

6.3 Prefragment shell structure

A common theme in all of this has been the importance of the underlying shell structure of the prefragments. Shell energy corrections were found to be important in $^{178}_{78}\text{Pt}_{100}$ and $^{180}_{80}\text{Hg}_{100}$; cluster formation in $^{294}_{118}\text{Og}_{176}$ was clearly influenced by the shell structure of the fragments; and the same may or may not be the case for $^{254}_{98}\text{Cf}_{156}$. Let's discuss this.

We used localizations to visualize the internal/intrinsic shell structure inside nuclei, and we were able to see that this structure was sometimes intact early in the evolution, at times as far back as the outer turning line. And actually, this kind of makes sense. From just energetics alone, a nucleus on the outer turning line is just as happy (or just as stable, or just as settled) as a nucleus in the ground state. In some sense, it is formed. The difference now is just that the configuration it's in is now unstable due to Coulomb. The two halves, which are kind of maybe happy from a nuclear physics perspective, are pushing apart from the Coulomb repulsion. So that still has to be carried out, but the bulk of the physics might already be done at this point - though not necessarily. It *could* be that the fragments are well-formed and just pushing apart, but that may not be the case. It's like a divorce: sometimes the two have drifted so far apart, or are so well-defined and incompatible as individuals that the divorce is simple and relatively straightforward. Other times, it is a mess trying to sort out who gets what, and the two parties are fundamentally-changed by the proceedings.

I don't have any strong objections to Scamps and Simenel's octupole paper. In fact, to me it kind of makes sense: we've been saying, after all, that it's the shell structure of the deformed prefragments which determine scission, and not necessarily the final fragments themselves. That's really the whole idea behind the localization paper: we're seeing that, at least in some cases, the shell structure is pretty well intact early in the evolution, and that

those prefragments drive the system to scission with some shuffling of the neck nucleons at scission. All they're saying is that those neck nucleons will affect the shell structure of the prefragments, and just based on the kinds of shapes that the system will take (small neck connecting two elongated or spherical fragments), the prefragments have a strong octupole moment (regardless of whether the fragments are elongated or spherical). So it shouldn't be the spherical magic numbers we worry about, but the deformed (in this case, octupole-deformed) magic numbers.

I feel like it shouldn't be too terrible to investigate this claim. What if we constrained the multipole moment(s) that correspond(s) to octupole-deformed fragments (perhaps Q_{50})? I think this parameter might be included in Peter Moller's model, but not in ours.

Chapter 7

Outlook

7.1 Review, outlook, and perspectives

In this chapter, it would be great to talk to everyone you know (Witek, Samuel, Jhila, Nicolas, Michal, and so on) to get a better feel for what kinds of issues need to be addressed next. You’ve already got sort of a rudimentary understanding (see your Google Keep note for starters), but it might be good to get some outsider perspective. This will be especially important as you start looking for postdocs, and *especially* especially if you end up looking for postdocs in nuclear theory, but not necessarily nuclear fission.

As I said in chapter 1, “Finally, in chapter 7 we discuss the current state of the field, and, based on our experience, offer insights for guiding future developments in the field.”

At this stage, we have techniques to calculate half-lives and primary fragment distributions (I haven’t mentioned it yet, but there is also Nicolas’ method for the fragment yields that uses TD-GCM. Are there others? What about for half-lives?). Some methods (such as Walid’s, TDDFT, and possibly also this GCM method) are starting to estimate fragment energetics (kinetic and excitation energies). Down the line, there are others who try to predict neutron multiplicities and goodness knows what else using Hauser-Feshbach models and such (FREYA and more). These regions are still disconnected. Of course, these methods still need major refinements in order to better reflect experimental data. Some ideas currently in

the pipeline for improving the models are:

- Improved EDFs (here you could mention the DME EDFs)
- Improved inertia tensor (such as automatic differentiation)
- Better/more collective coordinates (Walid's D, ξ coordinates or whatever they were called [Technical Report LLNL-TR-586678 (2012) Fragment yields calculated in a time-dependent microscopic theory of fission]; continuity of the PES in ∞ -dimensional space such like in David Regnier's talks and papers)
- Fragment identification (our localization paper, Marc Verriere's method; you might also mention that this is not an issue in TDDFT, but there you've only got one single fragment pair)
- Microscopic/self-consistent description for dissipation. This is the mechanism which exchanges between intrinsic and collective degrees of freedom, but we handle it in a very ad hoc way with parameters which are fitted instead of determined systematically through some theory. Solving this problem will probably help us with the energetics of fragments (TKE and E^* at the same time!)

Furthermore, there are more experimental observables that we should try to predict (refer to Andreyev's review to see what other observables can currently be measured). These include energetics (TKE and E^* , for we have only begun to scratch the surface here), angular momentum, prompt neutron multiplicities (is that within the scope of these self-consistent models?), prompt neutron and gamma energy spectra spectra (getting harder; these are usually handled via statistical models; see intro to [?] for some references), level densities?,

and probably more but my mind is blanking. How to compute these in a self-consistent framework is still an open question. See also the outlook in Nicolas' review.

We definitely need a better handle on the inertia. The perturbative inertia is easy to compute, but not terribly reliable. The non-perturbative inertia can certainly do better, but as it is computed now (using finite differences) it is subject to numerical artifacts and instabilities (dependent on the level of convergence of the individual densities, the coefficient multipliers, different basis sizes) and actual physics, such as level crossings which manifest in projections from a higher-dimensional space.

UNEDF1 seems to underestimate fission barrier heights (artificial though the concept may be; the main impact is probably that lifetimes are underestimated). It also turns out to be a headache to work with, making convergence quite a challenge sometimes (any cases in particular, like for highly-deformed or heavy or octupole-deformed nuclei or something?). Better functionals might hope to better capture the physics, and one can hope they are easier to work with.

APPENDIX

Appendix

Temperature-Dependent ATDHFB

Collective Inertia

.1

Everything which was shown in this dissertation assumed that the system was maintained at temperature $T = 0$ and the nucleus behaved as a superfluid below the Fermi surface. However, in many environments (such as a neutron star merger or a nuclear blast) there may be quite a bit of excitation energy imparted to the system, which would raise the temperature above the Fermi surface. In this case, pairs may be broken and the topology of the potential energy surface may change (see, for instance, [23]). In this case, the collective inertia of the system is changed, too, as shown below.

BIBLIOGRAPHY

BIBLIOGRAPHY

- [1] A. N. Andreyev, J. Elseviers, M. Huyse, P. Van Duppen, S. Antalic, A. Barzakh, N. Bree, T. E. Cocolios, V. F. Comas, J. Diriken, D. Fedorov, V. Fedosseev, S. Franchoo, J. A. Heredia, O. Ivanov, U. Köster, B. A. Marsh, K. Nishio, R. D. Page, N. Patronis, M. Seliverstov, I. Tsekhanovich, P. Van den Bergh, J. Van De Walle, M. Venhart, S. Vermote, M. Veselsky, C. Wagemans, T. Ichikawa, A. Iwamoto, P. Möller, and A. J. Sierk. New type of asymmetric fission in proton-rich nuclei. *Phys. Rev. Lett.*, 105(25):252502, Dec. 2010.
- [2] A. N. Andreyev, M. Huyse, and P. Van Duppen. Colloquium : Beta-delayed fission of atomic nuclei. *Rev. Mod. Phys.*, 85(4):1541–1559, Oct. 2013.
- [3] A. N. Andreyev, K. Nishio, and K.-H. Schmidt. Nuclear fission: a review of experimental advances and phenomenology. *Reports Prog. Phys.*, 81(1):016301, Jan. 2018.
- [4] A. Baran. Some dynamical aspects of the fission process. *Phys. Lett. B*, 76(1):8–10, May 1978.
- [5] A. Baran, K. Pomorski, A. Lukasiak, and A. Sobiczewski. A dynamic analysis of spontaneous-fission half-lives. *Nucl. Phys. A*, 361(1):83–101, May 1981.
- [6] A. Baran, J. A. Sheikh, J. Dobaczewski, W. Nazarewicz, and A. Staszczak. Quadrupole collective inertia in nuclear fission: Cranking approximation. *Phys. Rev. C*, 84(5):054321, Nov. 2011.
- [7] J. Bartel, P. Quentin, M. Brack, C. Guet, and H.-B. Håkansson. Towards a better parametrisation of skyrme-like effective forces: A critical study of the skm force. *Nucl. Phys. A*, 386(1):79–100, Sept. 1982.
- [8] M. Bender, P.-H. Heenen, and P.-G. Reinhard. Self-consistent mean-field models for nuclear structure. *Rev. Mod. Phys.*, 75(1):121–180, Jan. 2003.
- [9] J. Berger, M. Girod, and D. Gogny. Constrained hartree-fock and beyond. *Nucl. Phys. A*, 502:85–104, Oct. 1989.
- [10] N. Bohr and J. A. Wheeler. The mechanism of nuclear fission. *Phys. Rev.*, 56(5):426–450, Sept. 1939.
- [11] M. Brack, J. Damgaard, A. S. Jensen, H. C. Pauli, V. M. Strutinsky, and C. Y. Wong. Funny hills: The shell-correction approach to nuclear shell effects and its applications to the fission process. *Rev. Mod. Phys.*, 44(2):320–405, Apr. 1972.

- [12] R. Brandt, S. G. Thompson, R. C. Gatti, and L. Phillips. Mass and energy distributions in the spontaneous fission of some heavy isotopes. *Phys. Rev.*, 131(6):2617–2624, Sept. 1963.
- [13] N. T. Brewer, V. K. Utyonkov, K. P. Rykaczewski, Y. T. Oganessian, F. S. Abdullin, R. A. Boll, D. J. Dean, S. N. Dmitriev, J. G. Ezold, L. K. Felker, R. K. Grzywacz, M. G. Itkis, N. D. Kovrizhnykh, D. C. McInturff, K. Miernik, G. D. Owen, A. N. Polyakov, A. G. Popeko, J. B. Roberto, A. V. Sabel’nikov, R. N. Sagaidak, I. V. Shirokovsky, M. V. Shumeiko, N. J. Sims, E. H. Smith, V. G. Subbotin, A. M. Sukhov, A. I. Svirikhin, Y. S. Tsyganov, S. M. Van Cleve, A. A. Voinov, G. K. Vostokin, C. S. White, J. H. Hamilton, and M. A. Stoyer. Search for the heaviest atomic nuclei among the products from reactions of mixed-cf with a ca48 beam. *Phys. Rev. C*, 98(2):024317, Aug. 2018.
- [14] A. Bulgac, S. Jin, K. Roche, N. Schunck, and I. Stetcu. Fission dynamics. June 2018.
- [15] G. Flerov and K. Petrjak. Spontaneous fission of uranium. *Phys. Rev.*, 58(1):89–89, July 1940.
- [16] R. Gherghescu, J. Skalski, Z. Patyk, and A. Sobiczewski. Non-axial shapes in spontaneous fission of superheavy nuclei. *Nucl. Phys. A*, 651(3):237–249, May 1999.
- [17] S. A. Giuliani and L. M. Robledo. Non-perturbative collective inertias for fission: A comparative study. *Phys. Lett. B*, 787:134–140, Dec. 2018.
- [18] O. Hahn and F. Strassmann. Über den nachweis und das verhalten der bei der bestrahlung des urans mittels neutronen entstehenden erdalkalimetalle. *Naturwissenschaften*, 27(1):11–15, Jan. 1939.
- [19] A. V. Karpov, V. I. Zagrebaev, Y. M. Palenzuela, and W. Greiner. Superheavy nuclei: Decay and stability. pages 1–11.
- [20] M. Kortelainen, J. McDonnell, W. Nazarewicz, P.-G. Reinhard, J. Sarich, N. Schunck, M. V. Stoitsov, and S. M. Wild. Nuclear energy density optimization: Large deformations. *Phys. Rev. C*, 85(2):024304, Feb. 2012.
- [21] V. Liberati, A. N. Andreyev, S. Antalic, A. Barzakh, T. E. Cocolios, J. Elseviers, D. Fedorov, V. N. Fedoseev, M. Huyse, D. T. Joss, Z. Kalaninová, U. Köster, J. F. W. Lane, B. Marsh, D. Mengoni, P. Molkanov, K. Nishio, R. D. Page, N. Patronis, D. Pauwels, D. Radulov, M. Seliverstov, M. Sjödin, I. Tsekhanovich, P. Van den Bergh, P. Van Duppen, M. Venhart, and M. Veselský. β -delayed fission and α decay of ^{178}tl . *Phys. Rev. C*, 88(4):044322, Oct. 2013.
- [22] J.-F. Martin, J. Taieb, A. Chatillon, G. Béliet, G. Boutoux, A. Ebran, T. Gorbienet, L. Grente, B. Laurent, E. Pellereau, H. Alvarez-Pol, L. Audouin, T. Aumann,

- Y. Ayyad, J. Benlliure, E. Casarejos, D. Cortina Gil, M. Caamaño, F. Farget, B. Fernández Domínguez, A. Heinz, B. Jurado, A. Kelić-Heil, N. Kurz, C. Nociforo, C. Paradela, S. Pietri, D. Ramos, J.-L. Rodríguez-Sánchez, C. Rodríguez-Tajes, D. Rossi, K.-H. Schmidt, H. Simon, L. Tassan-Got, J. Vargas, B. Voss, and H. Weick. Studies on fission with aladin. *Eur. Phys. J. A*, 51(12):174, Dec. 2015.
- [23] J. D. McDonnell, W. Nazarewicz, J. A. Sheikh, A. Staszczak, and M. Warda. Excitation-energy dependence of fission in the mercury region. *Phys. Rev. C*, 90(2):021302, Aug. 2014.
- [24] L. Meitner and O. R. Frisch. Disintegration of uranium by neutrons: a new type of nuclear reaction. *Nature*, 143(3615):239–240, Feb. 1939.
- [25] P. Möller, J. Randrup, and A. J. Sierk. Calculated fission yields of neutron-deficient mercury isotopes. *Phys. Rev. C*, 85(2):024306, Feb. 2012.
- [26] R. Navarro Pérez, N. Schunck, A. Dyhdalo, R. J. Furnstahl, and S. K. Bogner. Microscopically based energy density functionals for nuclei using the density matrix expansion. ii. full optimization and validation. *Phys. Rev. C*, 97(5):054304, May 2018.
- [27] D. Poenaru, W. Greiner, K. Depta, M. Ivascu, D. Mazilu, and A. Sandulescu. Calculated half-lives and kinetic energies for spontaneous emission of heavy ions from nuclei. *At. Data Nucl. Data Tables*, 34(3):423–538, May 1986.
- [28] D. N. Poenaru and R. A. Gherghescu. α decay and cluster radioactivity of nuclei of interest to the synthesis of $z=119, 120$ isotopes. *Phys. Rev. C*, 97(4):044621, Apr. 2018.
- [29] D. N. Poenaru, R. A. Gherghescu, and W. Greiner. Heavy-particle radioactivity of superheavy nuclei. *Phys. Rev. Lett.*, 107(6):062503, Aug. 2011.
- [30] D. N. Poenaru, R. A. Gherghescu, and W. Greiner. Cluster decay of superheavy nuclei. *Phys. Rev. C*, 85(3):034615, Mar. 2012.
- [31] D. N. Poenaru, R. A. Gherghescu, and W. Greiner. Heavy-particle radioactivity. *J. Phys. Conf. Ser.*, 436:012056, Apr. 2013.
- [32] D. N. Poenaru, R. A. Gherghescu, W. Greiner, and N. S. Shakib. *How Rare Is Cluster Decay of Superheavy Nuclei?*, pages 131–140. Springer International Publishing, Cham, 2015.
- [33] D. N. Poenaru and W. Greiner. *Cluster Radioactivity*, pages 1–56. Springer Berlin Heidelberg, Berlin, Heidelberg, 2010.
- [34] J. Randrup, P. Möller, and A. J. Sierk. Fission-fragment mass distributions from strongly damped shape evolution. *Phys. Rev. C*, 84(3):034613, Sept. 2011.

- [35] P. Ring and P. Schuck. *The Nuclear Many-Body Problem*. Springer-Verlag, New York, 1980.
- [36] G. Royer, R. K. Gupta, and V. Denisov. Cluster radioactivity and very asymmetric fission through compact and creviced shapes. *Nucl. Phys. A*, 632(2):275–284, Mar. 1998.
- [37] J. Sadhukhan, J. Dobaczewski, W. Nazarewicz, J. A. Sheikh, and A. Baran. Pairing-induced speedup of nuclear spontaneous fission. *Phys. Rev. C*, 90(6):061304, Dec. 2014.
- [38] J. Sadhukhan, K. Mazurek, A. Baran, J. Dobaczewski, W. Nazarewicz, and J. A. Sheikh. Spontaneous fission lifetimes from the minimization of self-consistent collective action. *Phys. Rev. C*, 88(6):064314, Dec. 2013.
- [39] J. Sadhukhan, W. Nazarewicz, and N. Schunck. Microscopic modeling of mass and charge distributions in the spontaneous fission of 240pu. *Phys. Rev. C*, 93(1):011304, Jan. 2016.
- [40] J. Sadhukhan, C. Zhang, W. Nazarewicz, and N. Schunck. Formation and distribution of fragments in the spontaneous fission of 240pu. *Phys. Rev. C*, 96(6):061301, Dec. 2017.
- [41] K. P. Santhosh and C. Nithya. Systematic studies of α and heavy-cluster emissions from superheavy nuclei. *Phys. Rev. C*, 97(6):064616, June 2018.
- [42] N. Schunck, J. D. McDonnell, J. Sarich, S. M. Wild, and D. Higdon. Error analysis in nuclear density functional theory. *J. Phys. G Nucl. Part. Phys.*, 42(3):034024, Mar. 2015.
- [43] N. Schunck and L. M. Robledo. Microscopic theory of nuclear fission: a review. *Reports Prog. Phys.*, 79(11):116301, Nov. 2016.
- [44] A. J. Sierk. Langevin model of low-energy fission. *Phys. Rev. C*, 96(3):034603, Sept. 2017.
- [45] V. Strutinsky. Shell effects in nuclear masses and deformation energies. *Nucl. Phys. A*, 95(2):420–442, Apr. 1967.
- [46] V. Strutinsky. “shells” in deformed nuclei. *Nucl. Phys. A*, 122(1):1–33, Dec. 1968.
- [47] M. Warda and J. L. Egido. Fission half-lives of superheavy nuclei in a microscopic approach. *Phys. Rev. C*, 86(1):014322, July 2012.
- [48] M. Warda and L. M. Robledo. Microscopic description of cluster radioactivity in actinide nuclei. *Phys. Rev. C*, 84(4):044608, Oct. 2011.

- [49] M. Warda, A. Staszczak, and W. Nazarewicz. Fission modes of mercury isotopes. *Phys. Rev. C*, 86(2):024601, Aug. 2012.
- [50] M. Warda, A. Zdeb, and L. M. Robledo. Cluster radioactivity in superheavy nuclei. *Phys. Rev. C*, 98(4):041602, Oct. 2018.
- [51] C. F. v. Weizsäcker. Zur theorie der kernmassen. *Zeitschrift für Phys.*, 96(7-8):431–458, July 1935.
- [52] W. Younes and D. Gogny. Microscopic calculation of pu240 scission with a finite-range effective force. *Phys. Rev. C*, 80(5):054313, Nov. 2009.
- [53] W. Younes and D. Gogny. Nuclear scission and quantum localization. *Phys. Rev. Lett.*, 107(13):132501, Sept. 2011.
- [54] C. L. Zhang, B. Schuetrumpf, and W. Nazarewicz. Nucleon localization and fragment formation in nuclear fission. *Phys. Rev. C*, 94(6):064323, Dec. 2016.
- [55] Y. L. Zhang and Y. Z. Wang. Systematic study of cluster radioactivity of superheavy nuclei. *Phys. Rev. C*, 97(1):014318, Jan. 2018.
- [56] Y. Zhu, R. T. Wollaeger, N. Vassh, R. Surman, T. M. Sprouse, M. R. Mumpower, P. Möller, G. C. McLaughlin, O. Korobkin, T. Kawano, P. J. Jaffke, E. M. Holmbeck, C. L. Fryer, W. P. Even, A. J. Couture, and J. Barnes. Californium-254 and kilonova light curves. *Astrophys. J.*, 863(2):L23, Aug. 2018.